# Heat transfer in shallow caves: influence of turbulent convection

# Heat transfer in shallow caves: influence of turbulent convection

**B Qaddah[1], L Soucasse[1], F Doumenc[2,3], S Mergui[2,3], P Rivière[1] and A Soufiani[1]**

[1]Laboratoire EM2C, CNRS, CentraleSupélec, Université Paris-Saclay, 8-10 rue Joliot Curie, 91192 Gif-sur-Yvette, France
[2]Laboratoire FAST, Université Paris-Saclay, CNRS, Université Paris-Saclay, F-91405, Orsay, France
[3]Sorbonne Université, UFR 919, 4 place Jussieu, F-75252, Paris Cedex 05, France

E-mail: baraa.qaddah@centralesupelec.fr

**Abstract.** The enhancement of the conservation conditions of cave paintings requires a detailed understanding of heat transfer in such cavities. This article presents a numerical investigation of turbulent free convection in a parallelepipedic cavity. Non-homogeneous wall temperatures are prescribed from a large-scale model taking into account external temperature fluctuations damped by heat diffusion in the rock massif above the cavity. Large Eddy Simulation is performed to solve the turbulent flow fields for a given wall temperature field corresponding to a Rayleigh number of 8.5 x $10^9$ . The outcomes of the model are analysed in terms of statistical mean. Results show complex large scale flow patterns with regions of high turbulent intensity. The Q-criterion is used to identify turbulent structures for an instantaneous flow field. Then we analyse the spatial distribution of the conductive heat flux at the walls to locate the regions with intense convection. We show that the conductive flux smaller than the wall-to-wall radiative flux in the major part of the cavity, and close to its value at some spots.

## 1. Introduction

Shallow caves, from a few meters to about ten meters below the ground surface, are sensitive to seasonal variations of the external temperature, although temperature fluctuations between cold and hot periods are still perceptible in these caves, they are strongly attenuated by the thickness of the massif overhanging the cave. In particular, the differences in depth between floor and vault or between different zones of the cavity lead to temperature inhomogeneities of a few tenths of degree between different points at the wall at a given time. This is sufficient to generate significant natural convection flows, as well as evaporation/condensation phenomena at the walls since the relative humidity in these cavities is most often very close to 100%. This climate regime corresponds to that of many decorated caves in France (Lascaux [1], Marsoulas, Pech Merle, Gargas [2]) and throughout the world (Takamatsuzuka Tumulus in Japan [3]). Since intense and prolonged periods of condensation are likely to degrade paintings, the understanding of heat and mass transfers in this type of cavity is mandatory for the preservation of cave paintings. Previous studies have investigated heat transfer in shallow cavities such as Lascaux either by assigning a constant heat transfer coefficient [4] or by computing natural convection [5] with a high Rayleigh number ($Ra \sim 10^8$) assuming that the flow is laminar. However, at this

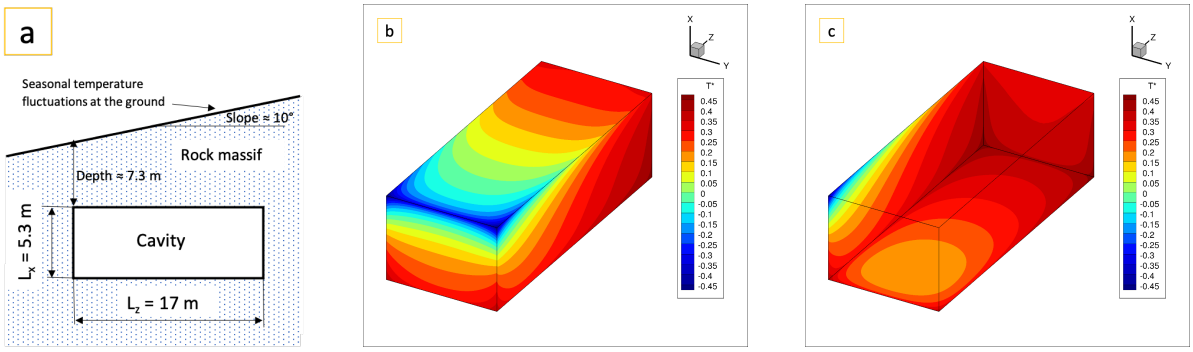


**Figure 1.** Geometry setup (a) and dimensionless temperature distribution (b and c) prescribed in the simulation and computed from a large-scale model [4] ($Ra = 8.5$ x $10^9$). $T^* = (T - T_0)/\Delta T$.

Rayleigh number, the flow is likely to be turbulent, at least in some part of the domain [6, 7]. Our objective is to highlight the influence of turbulent convection on heat transfer in a shallow cave, and to compare it with other heat transfer mechanisms. As a first step, we consider in this paper transparent air, and free convection is compared to wall-to-wall radiation.

## 2. Problem configuration

### *2.1. Geometry and boundary conditions*

We consider a parallelepiped cavity filled with air. The gravity acceleration field corresponds to $\boldsymbol{g} = -g\boldsymbol{x}$. The dimensions of the domain are $L_x = 5.3$m, $L_y = 1.32L_x$ and $L_z = 3.2L_x$. The floor and ceiling correspond to $x = 0$ and $x = L_x$ respectively, lateral walls correspond to $y = 0$ and $y = L_y$, and left and right walls correspond to $z = 0$ and $z = L_z$. The cavity, shown in figure 1-a and computed in a large-scale model [4] taking into account heat conduction in the rock and radiative transfer between the cave walls, was embedded in a massif with an upper surface inclined at 10° to the horizontal direction and the cavity upper edge is located at a depth of 7.3m from the ground surface. The boundary conditions in the present paper are no slip for the velocity and non-homogeneous temperature distribution for the six cave walls shown in figure 1(b-c) obtained from this model [4]. The maximum temperature difference is $\Delta T = (T_{max} - T_{min}) = 0.492$K and the reference temperature is $T_0 = (T_{max} + T_{min})/2 = 284.88$K.

### *2.2. Governing equations and numerical method*

Large Eddy Simulation (LES) is used in this study to save computational time. The spectral vanishing viscosity (SVV) method is implemented to provide numerical scheme stabilization [8]. The dimensionless governing equations, under Boussinesq approximation are given by:

$$\boldsymbol{\nabla}^*.\overline{\boldsymbol{u}}^* = 0, \tag{1}$$

$$\frac{\partial \overline{\boldsymbol{u}}^*}{\partial t^*} + \overline{\boldsymbol{u}}^*.\boldsymbol{\nabla}^*\overline{\boldsymbol{u}}^* = -\boldsymbol{\nabla}^*\overline{p}^* + Pr\overline{T}^*\boldsymbol{x}^* + \frac{Pr}{Ra^{0.5}}\boldsymbol{\nabla}^{*2}_{S_{VV}}\overline{\boldsymbol{u}}^* \tag{2}$$

$$\frac{\partial \overline{T}^*}{\partial t^*} + \overline{\boldsymbol{u}}^*.\boldsymbol{\nabla}^*\overline{T}^* = \frac{1}{Ra^{0.5}}\boldsymbol{\nabla}^{*2}_{S_{VV}}\overline{T}^*, \tag{3}$$

Where $\overline{a}^*$ is the dimensionless filtered variable and $\boldsymbol{\nabla}^{*2}_{S_{VV}}$ is the Laplacian operator modified by the SVV method. $Pr = \nu/\alpha = 0.712$, and $Ra = g\beta\Delta T L_x^3/(\alpha\nu) = 8.5 \times 10^9$ are respectively Prandtl number, and Rayleigh number. $\alpha$, $\nu$, $\beta$, $\boldsymbol{u}$, $p$, $T$ are thermal diffusivity, kinematic viscosity, thermal expansion coefficient, velocity vector, pressure and temperature,

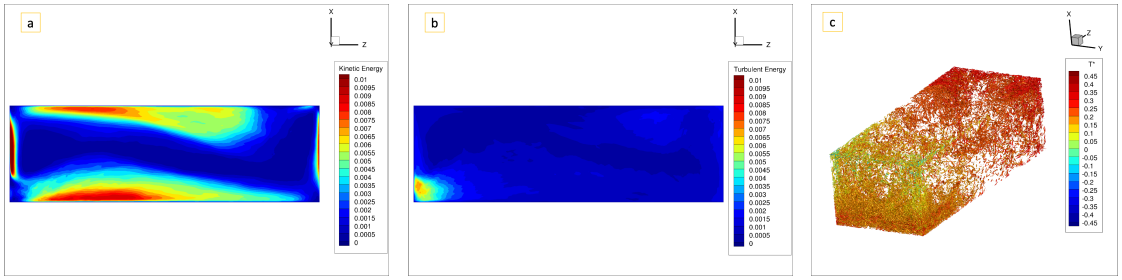


**Figure 2.** Kinetic energy of the mean flow $< \overline{u}_i^* >< \overline{u}_i^* > /2$ (a) and turbulent kinetic energy $< \overline{u}_i^{*'} \overline{u}_i^{*'} > /2$ (b) in the y* mid-plane. Where $< . >$ denotes the time average. Isosurfaces of the Q-criterion $[\Omega_{ij}\Omega_{ij} - S_{ij}S_{ij}\ ]/2$ ($Q = 10$) coloured by the temperature for an instantaneous flow field (c).

respectively. Equations are made dimensionless using the reference height $L_x$, the reference time $= L_x^2/(\alpha Ra^{0.5})$ and the reduced temperature is $T^* = (T - T_0)/\Delta T$. The governing flow equations are implemented in a spectral code [9] using a Chebyshev collocation method for the three spatial dimensions. This algorithm decomposes the computational domain along the largest spatial direction (here z-horizontal direction) in order to perform parallel computations [10]. The mesh size used here is $N_x \times N_y \times (N_z \times N_p) = 240 \times 240 \times (20 \times 32)$. Sensitivity analysis on spatial mesh size and SVV parameters have been performed to ensure results robustness.

## 3. Results

The main part of our numerical result is presented in the term of the statistical mean of variables over a dimensionless time period of about 100. This latter is taken once the sum of the integrated conductive flux over the surface of the six walls of the cavity reaches almost zero.

### *3.1. Flow field*

Figure 2-a shows the kinetic energy of the mean flow in the y* mid-plane. A large-scale circulation settles in the cave, with vertical flows along the left and right planes and horizontal flows along the floor and the ceiling. The maximum velocity in the system is about of 0.26 (0.093 $m/s$) and is located in the left region of the cavity due to the large temperature difference between the upper and lower sides (cold and hot edges respectively). Figure 2-b illustrates the turbulent kinetic energy in the y* mid-plane. This energy is distributed throughout the fluid domain and is concentrated in the lower left region of the system where a hot upward flow is forced to change its direction as a result of the cold downward flow. In order to identify the turbulent structures, one visualizes the Q-criterion [11], comparing rotation and strain rates, in figure 2-c for an instantaneous flow field. Vortex are observed almost everywhere in the cavity.

### *3.2. Heat fluxes*

We present in figure 3-(a-b) the local heat transfer rates at the walls (conductive flux $q_{cc}^* = -\boldsymbol{\nabla} T^* . \boldsymbol{n_{int}}$). We see this quantity is significant in the zones of intense convection, in particular on the upper left, upper lateral and lower right edges. Afterwards, we compare $q_{cc}^*$ with the radiative flux between the walls $q_{rad}^*$, assuming all walls are black, in figure 3 c-d and the total flux at the walls ($q_{tot}^* = q_{cc}^* + q_{rad}^*$) in figure 3 e-f. The radiative fluxes dominate the system and the convective flux remains important altering the sum of the fluxes in several spots (see figure 3-e-f), especially, at the floor, the lower parts of the walls and the right wall of the cavity. The maximum total heat flux in the system reaches 1 W/m$^2$.

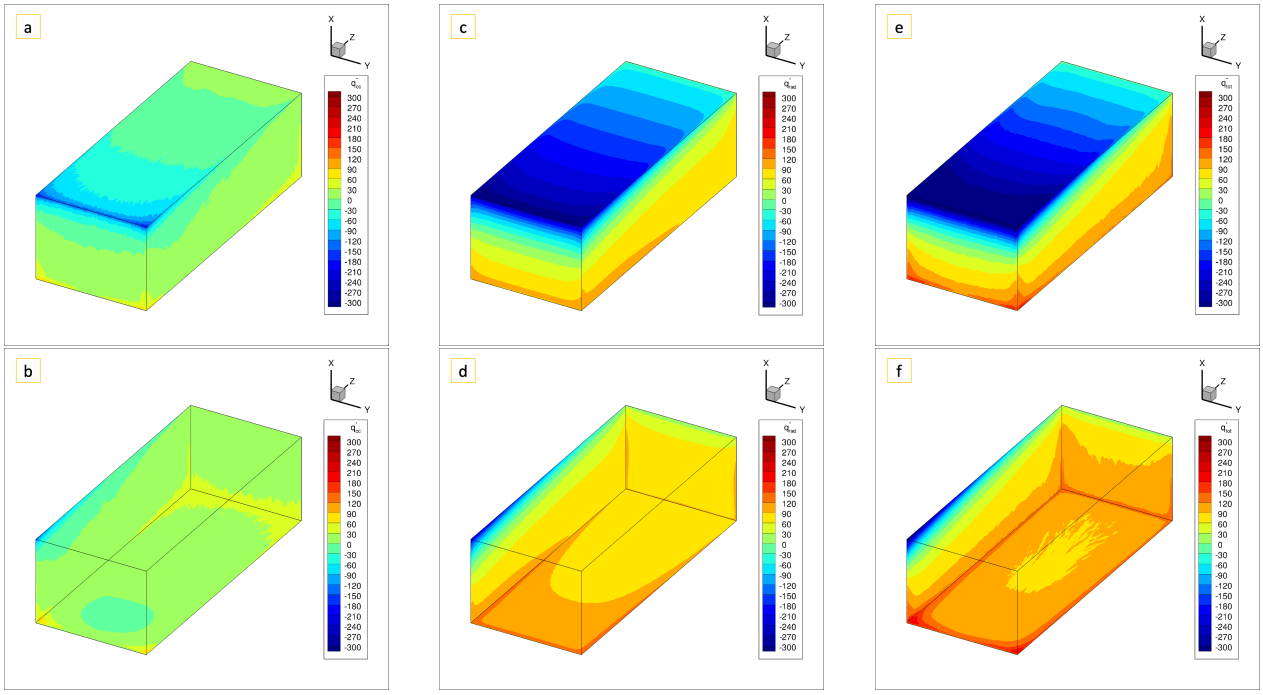


**Figure 3.** Heat fluxes at the walls of the cavity. a and b: conductive flux $q^*_{cc}$. c and d: wall-to-wall radiative flux $q^*_{rad}$. e and f: $q^*_{tot} = q^*_{cc} + q^*_{rad}$.

## 4. Conclusion

The effect of turbulent convective flow on heat transfer within an underground cavity has been investigated using large eddy simulations based on the spectral vanishing viscosity method. Using non-homogeneous wall temperatures, representative of external climate condition at a given moment of the year, we found that the turbulent kinetic energy is distributed over almost the whole fluid domain and that the vortex structures are concentrated in the regions receiving vertical convective flows. It is observed that the conductive fluxes at the wall are significant in the intense convection zones. Heat transfer at the cavity walls is mainly radiative. Convection is comparable to radiation at some localized spots, and negligible in the major part of the cavity. In a future work, we will consider a semi-transparent gas radiation (H2O, CO2), and the coupling with mass transport of water vapour will be taken into account in order to predict condensation and evaporation fluxes at the walls.

## References

[1] Houillon N, Lastennet R, Denis A, Malaurent P, Minvielle S and Peyraube N 2017 *Environ Earth Sci* **76** 170
[2] Bourges F, Genthon P, Genty D, Lorblanchet M, Mauduit E and D'Hulst D 2014 *Sci. of The Tot. Envi.* **493** 79–91
[3] Li Y, Ogura D, Hokoi S, Wang J and Ishizaki T 2014 *Journal of Asian Architecture* **13**
[4] Guerrier B, Doumenc F, Roux A, Mergui S and Jeannin P Y 2019 *Int. J. of Thermal Sciences* **146** 106066
[5] Lacanette D, Vincent S, Sarthou A, Malaurent P and Caltagirone J 2009 *Int. J. of Heat and Mass Trans.* **52** 2528–2542
[6] Pallares J, Cuesta I and Grau F 2002 *International Journal of Heat and Fluid Flow* **23** 346–358
[7] Soucasse L, Rivière P, Soufiani A, Xin S and Quéré P L 2014 *Physics of Fluids* **26** 024105
[8] Pasquetti R 2006 *Journal of Scientific Computing* **27** 365–375
[9] Xin S and Quéré P L 2002 *International Journal for Numerical Methods in Fluids* **40** 981–998
[10] Xin S, Chergui J and Quéré P L 2010 *In Parallel Computational Fluid Dynamics* **74** 163–171
[11] Wu-Shung F, Yu-Chih L and Chung-Gang L 2013 *Int. Communi. in Heat and Mass Trans.* **45** 41–46